NJC

ROYAL SOCIETY OF CHEMISTRY

PAPER

View Article Online
View Journal | View Issue

Check for updates

Cite this: *New J. Chem.*, 2025, **49**, 8279

Effect of the number and position of substituents on the orientation and sensor response of triethylene glycol-substituted silicon phthalocyanine films to ammonia

Victoria Ivanova, [a] Tamara Basova, *[a] Darya Klyamer, [a] Aleksandr Sukhikh, [a] Sebile Işık Büyükekşi, [b] Devrim Atilla [b] and Ayşe Gül Gürek *[b]

Received 6th February 2025,
Accepted 21st April 2025

DOI: 10.1039/d5nj00507h

rsc.li/njc

Si(IV)Pc derivatives bearing two $-O(CH_2CH_2O)_3CH_3$ substituents in axial positions (**SiPc-1**) and four (**SiPc-2**) or eight (**SiPc-3**) $-O(CH_2CH_2O)_3CH_3$ substituents on the phthalocyanine ring were investigated to reveal the effect of position and number of substituents on the orientation and chemiresistive sensor response of their films to ammonia. The liquid crystalline behavior of the Si(IV)Pc derivatives was studied using differential scanning calorimetry and polarizing optical microscopy. Only the **SiPc-3** derivative was found to exhibit a mesophase over a wide temperature range, identified as a discotic columnar hexagonal (Col_h) phase. The orientation of SiPc films prepared by spin coating was determined by polarized Raman spectroscopy. **SiPc-1** formed crystalline films with a preferential orientation of phthalocyanine macrocycles relative to the substrate surface, with the inclination angle of approximately 65°. **SiPc-2** films, on the other hand, were disordered. The introduction of eight triethylene glycol-substituents into **SiPc-3** resulted in a change in the film orientation, with the macrocycles oriented parallel to the substrate surface. **SiPc-3** films exhibited the best chemiresistive sensor response to ammonia, with a detection limit of 100 ppb and low response and recovery times.

Open Access Article. Published on 30 April 2025. Downloaded on 8/16/2025 7:57:06 PM.
This article is licensed under a Creative Commons Attribution-NonCommercial 3.0 Unported Licence.

1. Introduction

Metal phthalocyanines (MPcs) are of great interest to researchers due to a number of interesting spectral, optoelectronic and semiconductor properties. They are used not only as dyes,[1] catalysts[2] and photosensitizers,[3] but also as active layers in various devices, for example, electrochromic devices,[4] optical limiters,[5] in data storage media,[6] and chemical sensors.[7–9] MPcs are of interest as gas-sensitive materials capable of exhibiting an optical or resistive response to gases such as NO_2, Cl_2, NH_3, H_2S, and volatile organic compounds (VOCs).

The solubility of Pcs is an important factor that not only contributes to the preparation of thin layers by simple solution methods but also determines their physical and chemical properties. The solubility of Pcs in organic solvents can be improved by introducing various functional groups into peripheral and non-peripheral positions.[10–12] Along with improving solubility, the nature of substituents influences the sensor properties of MPcs. For examples, Şahin *et al.* investigated the effect of substituents (hexyl sulfanyl, hexyl sulfonyl and *p*-carboxyphenoxy) in NiPc derivatives on the sensor response of their layers in electrical sensor acting on the principles of an organic heterojunction effect.[13] Kilinç *et al.*[14] demonstrated that an increase in the length of substituents in lutetium bisphthalocyanines Lu(III)$(Pc(SC_nH_{2n+1})_4)_2$ (n = 6, 10, and 16) led to a decrease in the value of chemiresistive response to nitrogen dioxide when the response was measured at 25 °C but to its decrease when the sensing layers were heated to 150 °C. According to the authors' opinion this effect was due to the phase transition of lutetium bisphthalocyanines from the crystalline to liquid crystalline phase. Similar results were also observed by the same group of authors[15] when they studied the response of Lu(III)$(Pc(SC_nH_{2n+1})_4)_2$ (n = 6, 8, 10, 12, 16) films to several volatile organic compounds.

Several of our previous papers have also been devoted to studying the effect of the position and type of substituents on the chemiresistive sensor response of copper,[16] zinc[17] and lutetium[18] Pc films to gaseous ammonia. It was shown using the example of lutetium phthalocyanines bearing –OR or –SR substituents (R = $-CH_2CH_2O)_3CH_3$ that the derivatives with –SR have a higher response to NH_3 than those with –OR substituents. Alkylthio, alkyloxy and polyoxoethylene substituents in ZnPc and CuPc derivatives were shown to have a substantial

[a] *Nikolaev Institute of Inorganic Chemistry SB RAS, 3 Lavrentiev Pr., Novosibirsk, 630090, Russia. E-mail: tbasova@mail.ru*
[b] *Department of Chemistry, Faculty of Fundamental Sciences, Gebze Technical University, 41400, Gebze, Kocaeli, Turkey. E-mail: gurek@gtu.edu.tr*

Open Access Article. Published on 30 April 2025. Downloaded on 8/16/2025 7:57:06 PM.
This article is licensed under a Creative Commons Attribution-NonCommercial 3.0 Unported Licence.

effect on the liquid crystalline (LC) properties and as a consequence on the films ordering and their sensor response to ammonia. Pc derivatives that formed LC phases and more ordered films at room temperature demonstrated the higher chemiresistive response to ammonia.

Due to their aromatic structure, phthalocyanines can form supramolecular columnar ensembles. Some properties of Pcs strongly depend on the degree of intermolecular π–π interactions between the flat surfaces of macrocycles in such ensembles. Phthalocyanines of silicon(IV), germanium(IV), aluminum(III), gallium(III) and some other metals are of particular interest, since due to their degrees of oxidation they allow substituents to be introduced not only into the aromatic ring, but also into axial positions, which has a significant effect on intermolecular interactions and packaging of molecules and, as a result, on their properties.[19,20] Currently, a large number of axially substituted SiPc derivatives have been described, which can be obtained in the form of thin layers by various methods, namely by physical vapor deposition (PVD),[21] drop casting[22] or both,[23] which makes them suitable for investigation of electrical and sensor properties. Due to ligands in axial positions of SiPc molecules, these derivatives have different packing motifs in the solid than planar MPcs sometimes improving the π–π stacking required for efficient lateral charge transport and high charge carrier mobility.[24–26] SiPc has recently been shown to have promising application as n-type organic semiconductors or ambipolar semiconductors with other compounds incorporated into organic thin-film transistors (OTFTs),[26–28] organic light-emitting diodes[29,30] and organic solar cells.[31] There are a number of papers in the literature that analyze the effect of axial substitutes on the performance of organic thin-film transistors based on SiPc derivatives. Several studies show that the choice of the axial group affects the packing of SiPc in a single crystal, changing the stacking distance π–π, the herringbone angle and the degree of overlap of molecules.[24,32,33]

Despite the fact that various derivatives of SiPc are widely used, there are few works devoted to the study of their sensor properties. For instance, Fernandes *et al.*[34] studied chemiresistive sensor response of Langmuir–Blodgett films of *tert*-butyl silicon-[bis ethyloxy]-phthalocyanine (tbPcSi(OC_2H_5)$_2$) to nitrogen dioxide at a concentration of 5 ppm. The film's resistance increased in the atmosphere of NO_2, but its recovery was not very quick. The sensor properties of polymeric SiPc films were studied at high temperatures to detect gaseous NO_2 and Cl_2.[35] Bouvet with co-authors[36] used dichloro silicon phthalocyanine and bis(3,4,5 triflurophenoxy)silicon derivatives in organic heterojunction gas sensors for ammonia detection.[36] In our previous work, we prepared carbon nanotubes cross-linked through SiPc derivatives and studied their layers as sensors for detecting NH_3 and H_2.[37]

In this work, we study the effect of the number and position of triethylene glycol substituents on the orientation and chemiresistive sensor response of silicon phthalocyanine films to ammonia. The molecular structures of the investigated SiPc derivatives bearing two $-O(CH_2CH_2O)_3CH_3$ substituents in axial positions and four or eight $-O(CH_2CH_2O)_3CH_3$ substituents in the phthalocyanine ring are shown in Fig. 1.

2. Experimental details

2.1. Materials and films

SiPc-1, **SiPc-2** and **SiPc-3** derivatives were synthesized according to procedures previously described in the literature.[38,39] Films with a thickness of about 50 nm were deposited by spin coating of solutions (2 mg mL^{-1}) of SiPc derivatives in dichloromethane. For this purpose, a solution with a volume of 15 μL was dripped onto a substrate rotating at a speed of 2000 rpm. The thickness of the films was determined by spectral ellipsometry (spectral ellipsometer Ellips-1891, Russia).

2.2. Methods

Phase transition behavior of the compounds was observed with a polarizing microscope, Leitz Wetzler Orthoplan-pol, equipped with a hot stage Linkam TMS 93 and temperature-controller Linkam LNP. Temperatures of the phase transition were determined at scan rates of 5 °C min^{-1} using Mettler Toledo Star Thermal Analysis System/DSC 822 System differential scanning calorimeter calibrated with indium under a nitrogen atmosphere.

UV-vis spectra were recorded using a spectrophotometer CF 2000 (OKB Spectr, Russia). Raman spectra were recorded in back scattering geometry using a LabRAM Horiba single spectrometer (France) (488 nm line of an Ar+ laser) equipped with a microscope. AFM images were obtained using Ntegra Prima II nanolaboratory (NT-MDT, Moscow, Russia).

2.3. Study of the sensor properties

To measure chemiresistive sensor response films were deposited onto glass substrates with pre-deposited interdigitated platinum electrode (IDE). IDE (G-IDEPT10) were purchased from Metrohm, Spain. The resistance, which varied depending on the concentration of the analyzed gas, was measured using a Keithley 236 resistance meter at a constant voltage of 10 V and room temperature. The process included several stages. First, an air stream was blown into the chamber with the substrate until the constant resistance of the layer was reached. Then a gaseous analyte was introduced into the chamber at a given concentration (1–50 ppm), which caused a change in the resistance of the active layer. After that, the chamber was purged with air flow again until the resistance returned to its original value. The required concentration of gases in the test chamber was monitored using flow meters. Industrial dry ammonia from a cylinder provided by the company "Pure Gases" (Russia) was used as the source of the gaseous analyte.

3. Results and discussion

3.1. Study of mesogenic behaviour of Si(IV)Pc derivatives

The mesogenic phase behavior of Si(IV)Pc derivatives was studied using a combination of differential scanning calorimetry (DSC) and polarizing optical microscopy (POM). It was shown that among three investigated complexes, only **SiPc-3** demonstrated liquid crystal (LC) behavior. **SiPc-1** and **SiPc-2** were crystalline and did not from LC phase when heated (Fig. 2a and b). Fig. 2c presents the textures of the liquid crystalline

 This journal is © The Royal Society of Chemistry and the Centre National de la Recherche Scientifique 2025

Open Access Article. Published on 30 April 2025. Downloaded on 8/16/2025 7:57:06 PM.
This article is licensed under a Creative Commons Attribution-NonCommercial 3.0 Unported Licence.

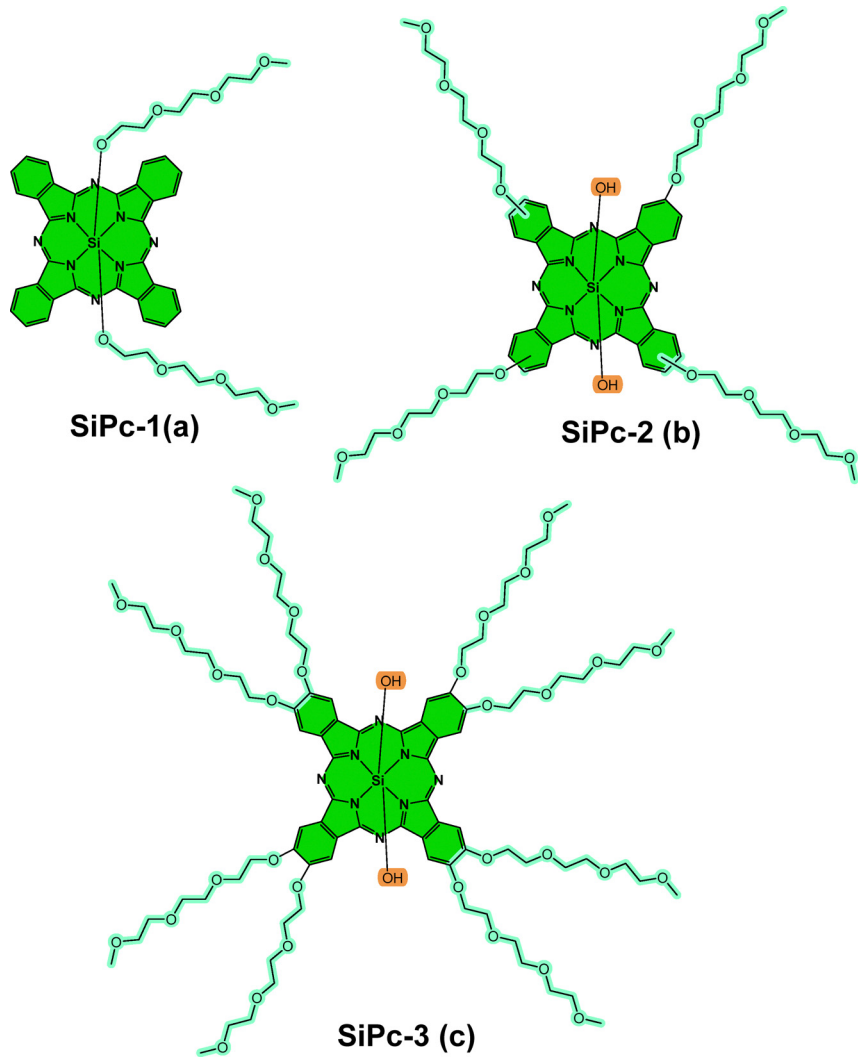

Fig. 1 Structures of Si(IV)Pc derivatives.

phases observed in POM under crossed polarizers. DSC results and polarizing microscopic observations for **SiPc-3** are listed in Table 1. **SiPc-3** forms only one type of a mesophase over a wide temperature range. When **SiPc-3** samples are heated at temperatures above 80 °C, a fan-shaped texture is observed under a polarizing microscope, which is usually characteristic of a columnar hexagonal ordering of the mesogens. This texture is similar to the texture described in the literature for other metal phthalocyanines forming a discotic hexagonal mesophase (Col_h).[40–43] When **SiPc-3** was cooled to room temperature, the

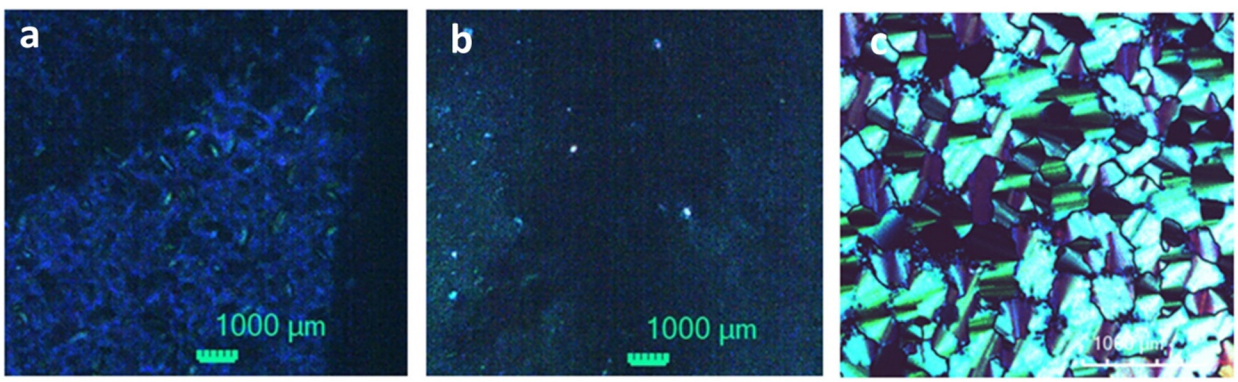

Fig. 2 Photomicrographs (under crossed polarizers) of **SiPc-1** (a), **SiPc-2** (b), and **SiPc-3** (c) at 50 °C.

Open Access Article. Published on 30 April 2025. Downloaded on 8/16/2025 7:57:06 PM.
This article is licensed under a Creative Commons Attribution-NonCommercial 3.0 Unported Licence.

Table 1 Phase transition temperatures for **SiPc-3**, determined by DSC (heating and cooling rates are 5 °C min^{-1}, heating range is from −40 to 250 °C)

Compound	Process	Liquid crystal (°C)	Decomposition (°C)
SiPc-3	Heating	−40 → 34	250
	Cooling	−15 ← 250	

optical texture of the mesophase was preserved. In the DSC study, one sharp peak was observed both when heated from −40 to 250 °C and when cooled from 250 to −40 °C (Table 1). The transition from the crystalline phase to the mesophase occurred at a temperature of about 34 °C during heating, and from the columnar mesophase back to the crystalline phase at about −15 °C during cooling. The heating cycle was interrupted before reaching the clearing point to avoid decomposition of the compound.

3.2. Characterization of SiPc films

UV-vis absorption spectra of SiPc films were compared with the spectra of their solutions in dichloromethane, as shown in Fig. 3. The spectra of solutions have a typical view for metal phthalocyanines and have B and Q bands. The Q bands, which are attributed to the doubly degenerate a_{1u}–e_g transition, are located at 672, 682 and 678 nm in the spectra of **SiPc-1**, **SiPc-2** and **SiPc-3** solutions. The Q band in the electronic absorption spectra of phthalocyanines is sensitive to both the aggregation of molecules in solution and the structural organization of thin films.[44] Based on its shape, it appears that all three SiPc

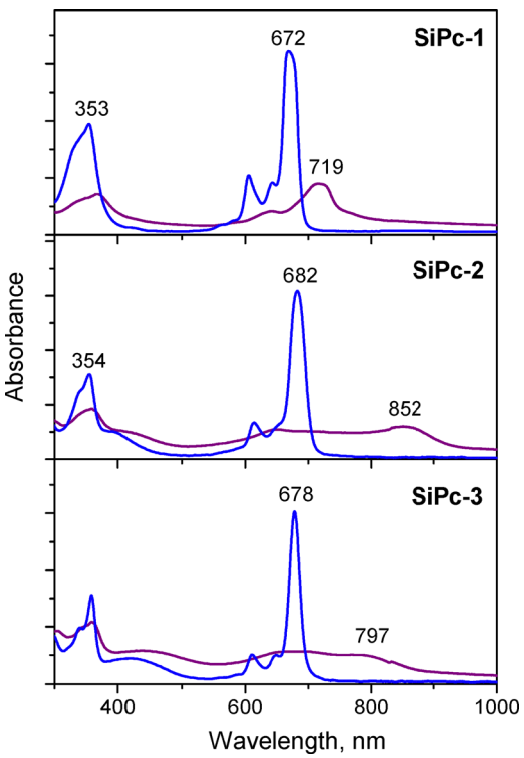

Fig. 3 Optical absorption spectra of **SiPc-1**, **SiPc-2** and **SiPc-3** solutions in dichloromethane (10^{-5} M, blue lines) and films (violet lines).

derivatives exist in monomeric forms in solutions. The spectra of SiPc films are broadened due to exciton coupling effects[45] and the Q bands exhibit a red shift, which is typical of a slipped-cofacially stacked configuration of macrocycles known as J-type aggregates.[46] The maximal red shift to 852 nm is observed for the spectrum of the **SiPc-2** film.

AFM images of **SiPc-1**, **SiPc-2** and **SiPc-3** films are shown in Fig. 4. The surface of the **SiPc-1** film is covered with individual sharp granules or crystallites, with a size of up to 0.5 μm. The root mean square (RMS) roughness of these films is approximately 10 nm. The surface of the **SiPc-2** and **SiPc-3** films is relatively smooth but covered with pinholes; the RMS roughness of both films is close to 3 nm.

The preferential orientation of SiPc macrocycles in thin films was investigated using polarized Raman spectroscopy. This technique has been previously used to study the molecular orientation of phthalocyanine films.[47–50] By measuring the ratio of the intensities of bands with a known type of symmetry in the spectra measured in parallel (ii) and cross (ij) polarizations of incident and scattered light, it is possible to determine whether the film has ordered structure and estimate the angle of inclination of molecules relative to the substrate surface. Raman spectra of SiPc films measured in parallel and cross polarizations of incident and scattered light are shown in Fig. 5. Assignment of vibrations by symmetry types was made based on symmetry types, using analogies with other phthalocyanines and the assumption that the phthalocyanine macrocycle has a D_{4h} symmetry group.[16,47] To verify reproducibility, the spectra were recorded at three different points on different sections of each film. The films turned out to be fairly homogeneous, and the difference in the intensity ratio of the bands, regardless of their symmetry type, was no more than 3%. Average values of the intensity ratio for A_{1g}, B_{1g}, and B_{2g} vibrations are presented in Table 2.

According to the analysis of the polarized Raman spectra, **SiPc-1** forms a crystalline film with the preferential orientation of phthalocyanine macrocycles relative to the substrate surface, with the inclination angle of about 65°. Such a type of orientation is typical for several crystalline phthalocyanine films.[51,52] The **SiPc-2** film was disordered because the measured I_{ii}/I_{ij} ratio was close to that of phthalocyanine solutions. The introduction of eight triethylene glycol-substituents to **SiPc-3** led to the change of its film orientation, with the molecules oriented parallel to the substrate surface. As shown above, **SiPc-3** exhibits LC behavior.

Researchers from the group of Prof. Lessard[49,50] also used polarized Raman spectroscopy to determine the inclination angle of molecules relative to the substrate surface in polycrystalline films of SiPc derivatives. It was found that the angle of macrocycle inclination in films of SiPc with tri-*n*-propylsilyloxy-substituents in axial positions was about 48°,[50] while in the case of SiPc with pentafluorooxy-substituents in axial positions, the angles varied from 28.8° to 38.8° in dependence on the type of template layer.[49]

It has been previously shown that heating phthalocyanine films exhibiting liquid crystal properties above their transition temperature to the mesophase resulted in the formation of

 This journal is © The Royal Society of Chemistry and the Centre National de la Recherche Scientifique 2025

Open Access Article. Published on 30 April 2025. Downloaded on 8/16/2025 7:57:06 PM.
This article is licensed under a Creative Commons Attribution-NonCommercial 3.0 Unported Licence.

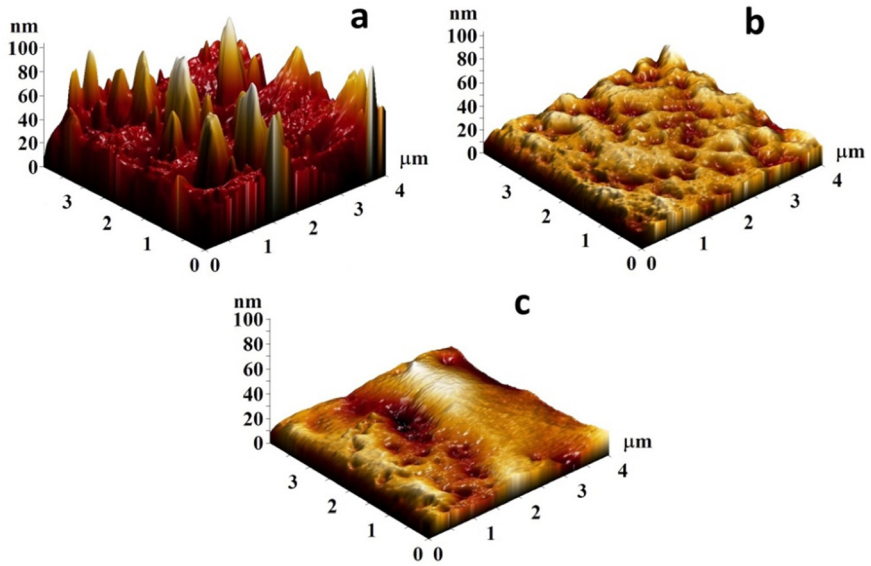

Fig. 4 AFM images of **SiPc-1** (a), **SiPc-2** (b) and **SiPc-3** (c) films.

aligned films. Most of the films obtained by heating mesogenic phthalocyanines on a single substrate were characterized by a perpendicular orientation of the macrocycles relative to the substrate surface, while spontaneous homeotropic alignment, in which the molecules lie parallel to the substrate, was observed only for some phthalocyanines. For example, discotic LC phthalocyanine with perfluorinated alkyl chains has been found to exhibit large area spontaneous homeotropic alignment on a variety of substrates. The spontaneous homeotropic alignment was also observed in the case of oxyphenyl substituted phthalocyanines $[C_nOPhO]_8Pc$.[53] According to the researchers, the parallel orientation of $[C_nOPhO]_8Pc$ macrocycles was induced by the stronger interaction between the lone pairs of oxygen atoms in the phenoxy group and the dangling bonds on the Si atoms of a substrate. In the case of **SiPc-3**, the parallel orientation of macrocycles can also be induced by a combination of a large number of oxygen atoms in $-O(CH_2CH_2O)_3CH_3$ substituents and –OH substituents in the axial positions.

The conclusion about the alignment of the films is also supported by the XRD data (Fig. 6). The diffraction pattern of the **SiPc-1** film has multiple strong diffraction peaks, including peaks at 3.96°, 7.97°, 15.96° and 24.03° 2θ, which appear to belong to the same set of crystallographic planes, *i.e.* (001), (002), (004) and (006). This indicates that the **SiPc-1** film has a noticeable preferred orientation along these crystallographic planes with the SiPc macrocycles inclined relative to the substrate surface.[54]

A **SiPc-3** diffraction pattern has only two diffraction peaks at 24.47° 2θ (3.64 Å) and 28.98° 2θ (3.08 Å), corresponding to the distances between the neighbor SiPc macrocycles in the stack and between the OH-group of one SiPc molecule and the neighbor SiPc macrocycle. This indicates a parallel orientation of the phthalocyanine macrocycles relative to the substrate surface in this film. The diffractogram of the **SiPc-2** does not show any pronounced peaks.

3.3. Sensor response of SiPc films to ammonia

The change in the resistance of SiPc films during alternating injection of ammonia at concentrations ranging from 1 to 50 ppm and air purging is shown in Fig. 7. The resistance of the **SiPc-1** and **SiPc-2** films increased when ammonia was injected into the cell, while the resistance of the **SiPc-3** films decreased. An increase in resistance in the atmosphere of electron donor gases, in particular ammonia, has been observed for p-type semiconductor films, which include most metal phthalocyanines.[55] For example, tetra-*tert*-butyl substituted SiPc with two $-OC_2H_5$ groups in axial positions[56] demonstrated p-type behavior when NO_2 was detected.

A decrease in resistance in the atmosphere of electron-donating gases is characteristic of n-type semiconductor films. It is known that metal phthalocyanines, depending on the type of substituent, can behave like n-type semiconductors. In some cases, they exhibit ambipolar properties. Among the phthalocyanines that exhibit n-type semiconductor behavior, $MPcF_{16}$ (M = Cu, Co)[55] and some derivatives of SnPc[57] and SiPc[26,33] have been widely studied.

The introduction of eight polyoxyethylene substituents in combination with OH groups in the axial positions of **SiPc-3** causes a change in the direction of resistance change in an ammonia atmosphere.

The process of adsorption of oxygen molecules on the surface of a phthalocyanine film during exposure to ambient air and their further substitution with ammonia molecules is usually considered as a mechanism of the sensor response.[58,59] Based on the results obtained regarding the conductivity type of the SiPc films, the mechanism of their sensor response to NH_3 can be described as follows. When oxygen molecules are adsorbed on the surface of the film, they attract electrons from SiPc. This attraction results in a decrease in electron concentration within the SiPc films. Consequently, for **SiPc-3**, electrical conductivity decreases, while for **SiPc-1** and **SiPc-2**, conductivity increases. Since O_2 molecules are nonpolar and weakly bound to the

Open Access Article. Published on 30 April 2025. Downloaded on 8/16/2025 7:57:06 PM.
This article is licensed under a Creative Commons Attribution-NonCommercial 3.0 Unported Licence.

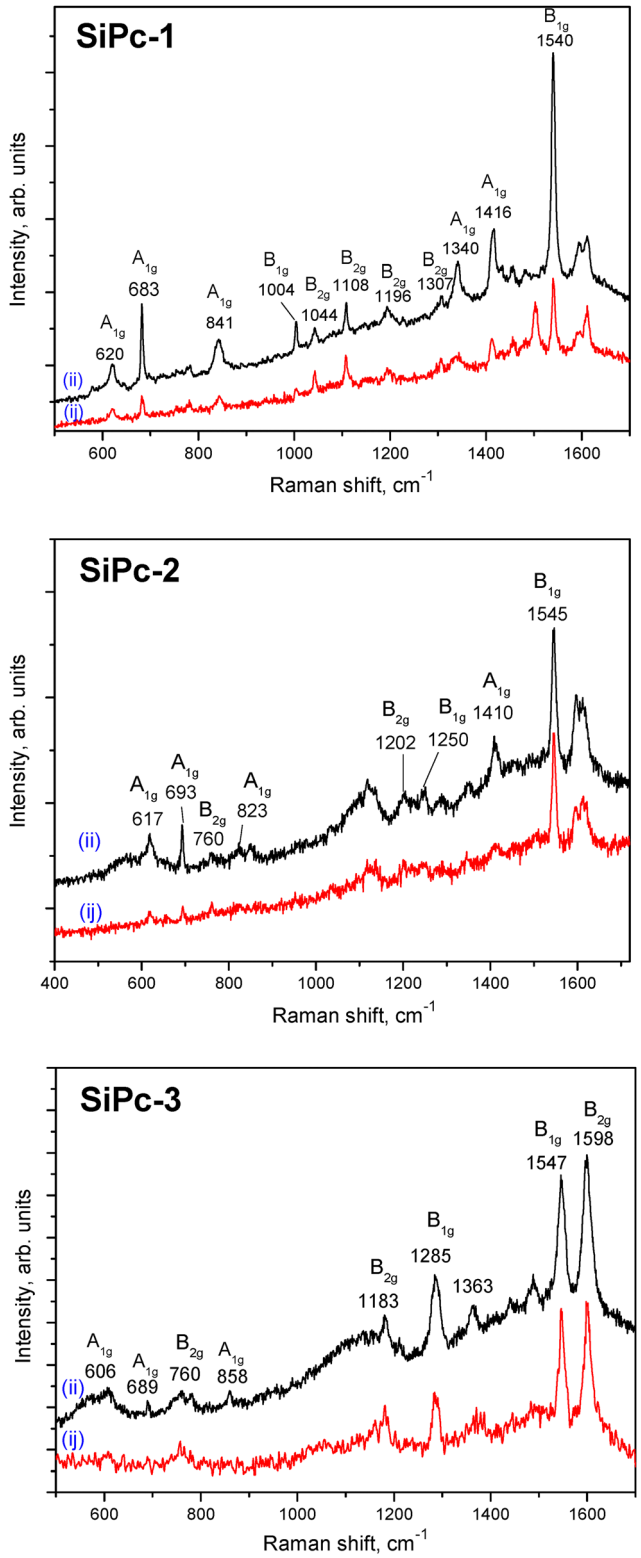

Fig. 5 Raman spectra of **SiPc-1**, **SiPc-2** and **SiPc-3** films measured in parallel (ii) and cross (ij) polarizations of incident and scattered light.

surface of the thin films, they can be easily displaced by polar molecules like NH_3. As a result, the electrons that were previously attracted by oxygen molecules are released back into the film. For **SiPc-3**, this process leads to an increase in conductivity (decrease in resistance as in Fig. 7), whereas for **SiPc-1** and **SiPc-2**, it results in a decrease in conductivity. It is important to note that ammonia is known to act as electron donors and its adsorption can further increase the concentration of electrons in the films.

Table 2 Measured I_{ii}/I_{ij} ratios for A_{1g}, B_{1g} and B_{2g} modes in the Raman spectra of **SiPc-1**, **SiPc-2** and **SiPc-3** films and calculated angles of molecule inclination

	I_{ii}/I_{ij} ratios for A_{1g}, B_{1g} and B_{2g} modes			
Films	A_{1g}	B_{1g}	B_{2g}	Orientation
SiPc-1	3.8	3.0	1.4	Ordered film inclination angle 65 ± 5°
SiPc-2	~5	1.4	1.4	Disordered film
SiPc-3	>20	1.0	1.0	Ordered film inclination angle is close to 0°

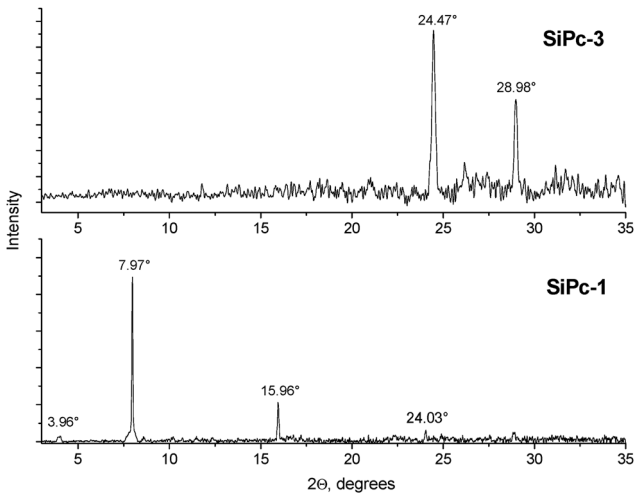

Fig. 6 XRD patterns of **SiPc-1** and **SiPc-3** films.

Since the resistance of one SiPc film increases and the resistance of another SiPc film decreases, the sensor response is defined as $S_{resp} = |R - R_o|/R_o$, where R_o is the base resistance, that is the resistance measured in air without exposure to the gaseous analyte, and R is the resistance of the layer after exposure to a certain concentration of the gaseous analyte. The sensor response of all investigated films was fully reversible at room temperature.

A comparison of the dependence of the sensor response on the concentration of ammonia for all three films is shown in Fig. 8. The standard deviations for each sample are indicated according to five parallel measurements. **SiPc-1** films exhibit linear dependence of the response over the entire investigated concentration range. The graphs for **SiPc-2** and **SiPc-3** film have two linear ranges with different slopes: from 1 to 10 ppm and from 10 to 50 ppm. **SiPc-3** films demonstrate the highest sensor response to ammonia among the investigated films. For example, S_{resp} of the **SiPc-3** film to 100 ppm NH_3 is 2.5 higher than that of **SiPc-2** and 4.4 times higher than that of **SiPc-1** (Fig. 8).

 This journal is © The Royal Society of Chemistry and the Centre National de la Recherche Scientifique 2025

Open Access Article. Published on 30 April 2025. Downloaded on 8/16/2025 7:57:06 PM.
This article is licensed under a Creative Commons Attribution-NonCommercial 3.0 Unported Licence.

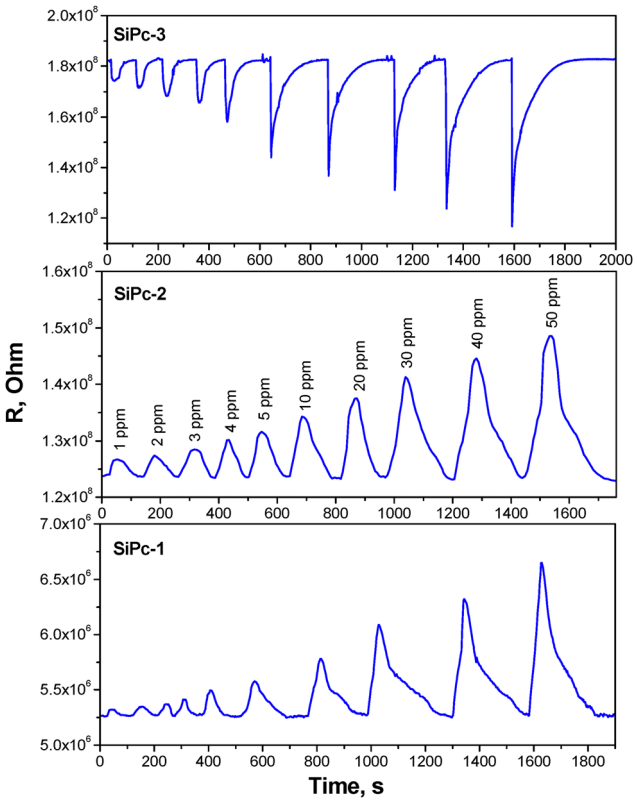

Fig. 7 The change in the resistance of **SiPc-1**, **SiPc-2** and **SiPc-3** films during alternating injection of ammonia with a concentration from 1 to 50 ppm and air purging. Measurements were carried out at room temperature.

The limits of detection (LOD) calculated as $3\sigma/m$ (where σ is the standard deviation of S_{resp} to 1 ppm NH_3 and m is the slope of the calibration curve in the range from 1 to 10 ppm) for **SiPc-1**, **SiPc-3** and **SiPc-3** films are given in Table 3. All investigated films have quite short response and recovery times.

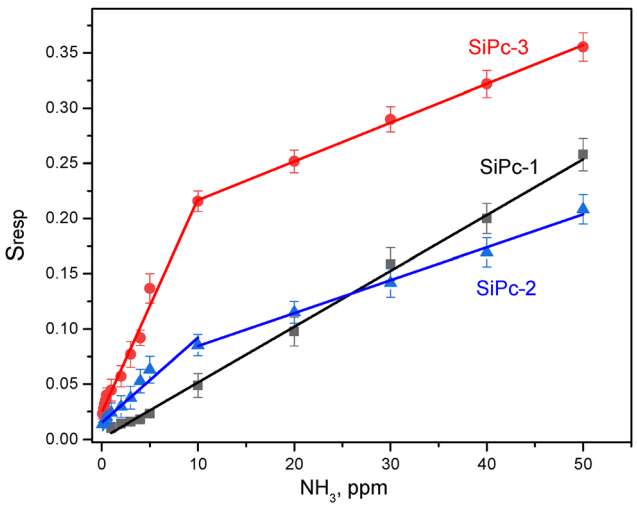

Fig. 8 Dependence of the sensor response of **SiPc-1**, **SiPc-2** and **SiPc-3** films on ammonia concentration. Measurements were carried out at room temperature.

Table 3 LOD, response and recovery times for **SiPc-1**, **SiPc-2** and **SiPc-3** films

Film	LOD to NH_3, ppm	Response time, s (to 5 ppm NH_3)	Recovery time, s (to 5 ppm NH_3)
SiPc-1	0.32	20	45
SiPc-2	0.28	30	70
SiPc-3	0.10	10	60

Thus, **SiPc-3**, which exhibit mesogenic behavior and form films with homeotropic alignment, demonstrates the maximal sensitivity to ammonia among three investigated silicon phthalocyanines. This increased sensitivity may be influenced by a combination of several factors. First, discotic liquid crystalline materials exhibit a more efficient overlap of π–π molecular orbitals within columnar stacks, leading to enhanced charge carrier mobility.[60] Consequently, the charge can more effectively move within the stack of discotic **SiPc-3**, leading to a significant and rapid change in resistance. Second, more number of molten polyoxoethylene substituents in **SiPc-3**, which contain more oxygen atoms and are capable of forming van der Waals contacts with NH_3 molecules, provides a larger number of active centers.

3.4. Performance of a SiPc-3-based sensor

More detailed sensor characteristics were studied using a **SiPc-3** film as an example. Repeatability and long-term stability are also important characteristics for the practical application of sensors. To study the sensor repeatability, the response of a **SiPc-3** film to repeated injections of 5 ppm NH_3 was measured over 95 min (Fig. 9a).

To study the long-term stability the response of the same film to 5 ppm of NH_3 was measured after 3, 39, 40, and 46 days (Fig. 9b). The change in the sensor response did not exceed the measurement error, which indicated good repeatability and long-term stability of the investigated **SiPc-3** film.

To assess the selectivity of the sensors, the response to ammonia was compared with that to gaseous H_2S, CO_2, vapors of dichloromethane, ethanol, acetone and water vapors. The sensor response to these gases and vapors is shown in Fig. 10, using a film of **SiPc-3** as an example. It can be seen that at low concentrations, volatile organic solvents and water do not interfere with the determination of ammonia, while their increase to several thousand ppm can lead to interference. At the same time, the film is insensitive to CO_2, but hydrogen sulfide, which is an electron-donating gas like ammonia, produces a sensor response similar to that of ammonia.

Sensor characteristics of the **SiPc-3** film in relation to ammonia were compared with those of other sensors based on different silicon phthalocyanine derivatives described in the literature, and phthalocyanines of zinc ($ZnPcR_8$) and lutetium ($Lu(PcR_8)_2$) with the same substituents R = $-O(CH_2CH_2O)_2CH_3$ in the macrocycle, which were studied in our previous works at the same experimental conditions as **SiPc-3** (Table 4). The **SiPc-3** films have a lower detection limit compared to sensors based on other silicon phthalocyanine films, but their detection limit is worse than that of a sensor based on the films of zinc phthalocyanine bearing the same substituents. However, the **SiPc-3** sensors have lower response and recovery times.

Open Access Article. Published on 30 April 2025. Downloaded on 8/16/2025 7:57:06 PM.
This article is licensed under a Creative Commons Attribution-NonCommercial 3.0 Unported Licence.

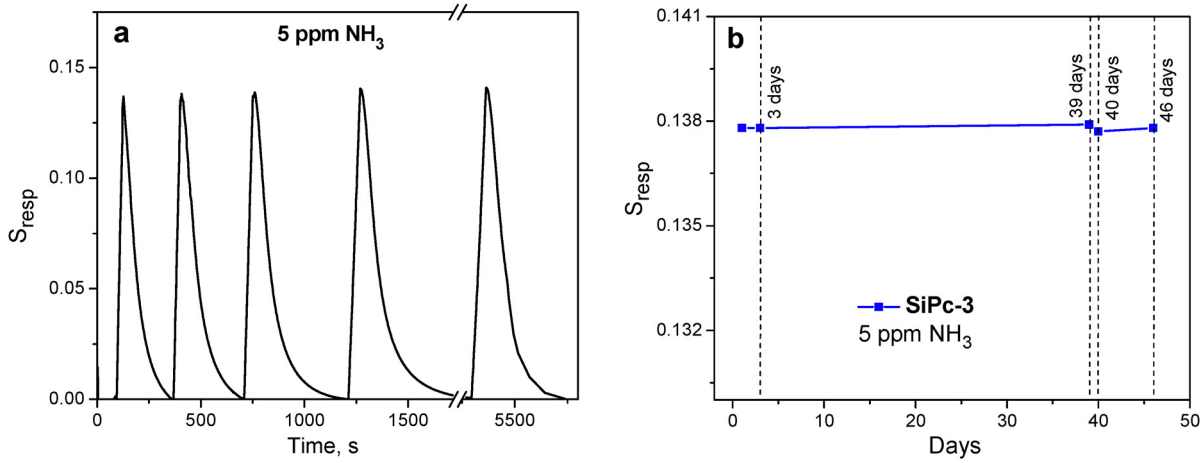

Fig. 9 The sensor response of a **SiPc-3** film to repeated injections of 5 ppm NH_3 (a) and the same film to 5 ppm NH_3 after 3, 39, 40, and 46 days (b).

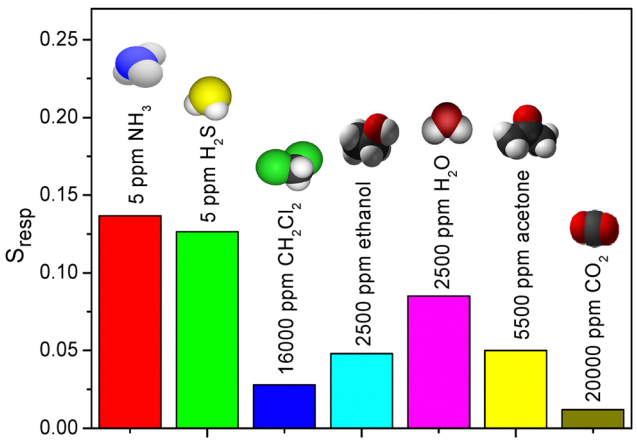

Fig. 10 Sensor response of a **SiPc-3** film to ammonia (5 ppm), hydrogen sulfide (5 ppm), dichloromethane (16 000 ppm), ethanol (2500 ppm), water vapor (2500 ppm), acetone (5500 ppm), and carbon dioxide (20 000 ppm).

4. Conclusions

SiPc derivatives bearing two $-O(CH_2CH_2O)_3CH_3$ substituents in axial positions and four or eight $-O(CH_2CH_2O)_3CH_3$ substituents in the phthalocyanine ring were investigated to reveal the effect of position and number of substituents on the orientation and chemiresistive sensor response of their films to low concentrations of ammonia (0.1–10 ppm). It was shown by the methods of DSC and POM that among investigated phthalocyanines, only **SiPc-3** bearing eight $-O(CH_2CH_2O)_3CH_3$ substituents in the macrocycle exhibited a mesophase in a wide temperature range. According to the analysis of the polarized Raman spectra, **SiPc-1** formed crystalline films with preferential orientation of phthalocyanine macrocycles relative to the substrate surface with the inclination angle of about 65°, whereas the **SiPc-2** films were disordered. The introduction of eight triethylene glycol-substituents to **SiPc-3** led to the change of its film orientation with the molecules oriented parallel to the substrate surface. All investigated films had the reversible sensor response to ammonia at room temperature. **SiPc-3** films exhibited the best chemiresistive sensor response to ammonia with the detection limit of 100 ppb, determined in the linear concentration range from 0.1 to 10 ppm, and low response and recovery times at 1 ppm NH_3 of 10 and 60 s, respectively. The detection limit of **SiPc-3** films for ammonia is much lower than the exposure limit to human (25 ppm) recommended by Occupational Safety and Health Administration (OSHA, https://www.osha.gov/chemicaldata/623) and the content of ammonia in the exhaled air of healthy individuals,[65] which makes these materials suitable for use as ammonia sensors for monitoring environmental pollution and exhaled air composition for non-invasive diagnosis of various diseases.

Author contributions

Victoria Ivanova: investigation, formal analysis, visualization, writing – original draft. Darya Klyamer: investigation, formal

Table 4 Sensor characteristics of ammonia sensors based on silicon phthalocyanine derivatives and metal phthalocyanines with triethylene glycol substituents

Layers	Sensor type	LOD ($3\sigma/m$), ppb	Linear range, ppm	Response time, s	Recovery time, s	Ref.
$(345F)_2SiPc/LuPc_2$	Organic heterojunction gas sensors	310	10–90	<60 (at 90 ppm)	<60 (at 90 ppm)	61
$Cl_2SiPc/LuPc_2$	Organic heterojunction gas sensors	100	10–90	<420 (at 90 ppm)	<420 (at 90 ppm)	61
$(F_5PhO)_2$-SiPc/$LuPc_2$	Organic heterojunction gas sensors	307	1–9	—	51	62
$(F_5PhO)_2$-F_4SiPc/$LuPc_2$		750	1–9	—	134	
$(F_5PhO)_2$-F_{16}SiPc/$LuPc_2$		618	1–9	—	60	
$Lu(PcR_8)_2$ R = $-O(CH_2CH_2O)_2CH_3$	Chemiresistive sensors	80	0.1–10	28 (at 1 ppm)	88 (at 1 ppm)	63
$ZnPcR_8$ R = $-O(CH_2CH_2O)_2CH_3$	Chemiresistive sensors	17	0.1–5	30 (at 1 ppm)	78 (at 1 ppm)	64
SiPc-3	Chemiresistive sensors	100	0.1–10	10 (at 1 ppm)	60 (at 1 ppm)	This work

 This journal is © The Royal Society of Chemistry and the Centre National de la Recherche Scientifique 2025

Open Access Article. Published on 30 April 2025. Downloaded on 8/16/2025 7:57:06 PM. This article is licensed under a Creative Commons Attribution-NonCommercial 3.0 Unported Licence.

analysis, validation, visualization, writing – original draft. Aleksandr Sukhikh: investigation, formal analysis, visualization, writing – original draft. Sebile Işık Büyükeksi: investigation, data curation, formal analysis. Devrim Atilla: methodology, writing – original draft, writing – review & editing. Ayşe Gül Gürek: methodology, writing – original draft, writing – review & editing, supervision. Tamara Basova: methodology, writing – original draft, writing – review & editing, supervision, funding acquisition. All authors have read and agreed to the published version of the manuscript.

Data availability

The data that support the findings of this study are available from the corresponding author upon reasonable request. The data are not publicly available due to participant privacy and ethical considerations. Any additional data or materials can be provided upon request to ensure transparency and reproducibility of the research.

Conflicts of interest

There are no conflicts to declare.

Acknowledgements

VI, DK and TB acknowledge Ministry of Education and Science of the Russian Federation for the financial support.

References

1 X. Song, R. Xu, Q. Yao, L. Tian, J. Li, B. Yang, P. Chen, J. Zhang, H. Xin and X. Peng, *Dyes Pigm.*, 2024, **228**, 112244.
2 J. Zhao, H. Lyu, Z. Wang, C. Ma, S. Jia, W. Kong and B. Shen, *Sep. Purif. Technol.*, 2023, **312**, 123404.
3 K. P. Channabasavana Hundi Puttaningaiah and J. Hur, *Inorg. Chem. Commun.*, 2024, **170**, 113491.
4 B. Yıldız, Ö. Budak, A. Koca and M. K. Şener, *Dyes Pigm.*, 2024, **223**, 111958.
5 A. Y. Tolbin, M. S. Savelyev, A. Y. Gerasimenko and L. G. Tomilova, *Chem. Phys. Lett.*, 2016, **661**, 269–273.
6 H. S. Majumdar, A. Bandyopadhyay and A. J. Pal, *Org. Electron.*, 2003, **4**, 39–44.
7 R. P. Reji, Y. Sivalingam, Y. Kawazoe and S. Velappa Jayaraman, *Mol. Syst. Des. Eng.*, 2024, **9**, 286–299.
8 V. Ivanova, A. Şenocak, D. Klyamer, E. Demirbas, S. Makhseed, P. Krasnov, T. Basova and M. Durmuş, *Sens. Actuators, B*, 2024, **398**, 134733.
9 C. P. Keshavananadaprabhu, S. Aralekallu and L. K. Sannegowda, *Adv. Sens. Res.*, 2024, 2400088.
10 Z. Biyiklioglu and O. Bekircan, *Synth. Met.*, 2015, **200**, 148–155.
11 Z. Biyiklioğlu, *Synth. Met.*, 2011, **161**, 508–515.
12 O. Bekircan, Z. Biyiklioğlu, I. Acar, H. Bektas and H. Kantekin, *J. Organomet. Chem.*, 2008, **693**, 3425–3429.
13 Z. Şahin, R. Meunier-Prest, F. Dumoulin, A. Kumar, Ü. Isci and M. Bouvet, *Sens. Actuators, B*, 2021, **332**, 129505.
14 N. Kilinç, D. Atilla, A. G. Gürek, Z. Z. Öztürk and V. Ahsen, *Sens. Actuators, B*, 2009, **142**, 73–81.
15 N. Kilinç, D. Atilla, A. G. Gürek, Z. Z. Öztürk and V. Ahsen, *Talanta*, 2009, **80**, 263–268.
16 A. D. Gülmez, M. S. Polyakov, V. V. Volchek, S. T. Kostakoğlu, A. A. Esenpinar, T. V. Basova, M. Durmuş, A. G. Gürek, V. Ahsen, H. A. Banimuslem and A. K. Hassan, *Sens. Actuators, B*, 2017, **241**, 364–375.
17 V. Ivanova, D. Klyamer, G. Tunç, F. D. Gürbüz, D. Atilla, A. G. Gürek, A. Sukhikh and T. Basova, *New J. Chem.*, 2023, **47**, 19633–19645.
18 H. Karakaş, V. Ivanova, G. G. Çelik, D. Atilla, A. G. Gürek, D. Klyamer and T. Basova, *Synth. Met.*, 2021, **281**, 116924.
19 K. Mitra and M. C. T. Hartman, *Org. Biomol. Chem.*, 2021, **19**, 1168–1190.
20 M. D. Maree and T. Nyokong, *J. Porphyrins Phthalocyanines*, 2001, **5**, 555–563.
21 B. King, O. A. Melville, N. A. Rice, S. Kashani, C. Tonnelé, H. Raboui, S. Swaraj, T. M. Grant, T. McAfee, T. P. Bender, H. Ade, F. Castet, L. Muccioli and B. H. Lessard, *ACS Appl. Electron. Mater.*, 2021, **3**, 325–336.
22 B. H. Lessard, *ACS Appl. Mater. Interfaces*, 2021, **13**, 31321–31330.
23 R. R. Cranston, B. King, C. Dindault, T. M. Grant, N. A. Rice, C. Tonnelé, L. Muccioli, F. Castet, S. Swaraj and B. H. Lessard, *J. Mater. Chem. C*, 2022, **10**, 485–495.
24 B. H. Lessard, T. M. Grant, R. White, E. Thibau, Z.-H. Lu and T. P. Bender, *J. Mater. Chem. A*, 2015, **3**, 24512–24524.
25 B. H. Lessard, R. T. White, M. AL-Amar, T. Plint, J. S. Castrucci, D. S. Josey, Z.-H. Lu and T. P. Bender, *ACS Appl. Mater. Interfaces*, 2015, **7**, 5076–5088.
26 O. A. Melville, T. M. Grant and B. H. Lessard, *J. Mater. Chem. C*, 2018, **6**, 5482–5488.
27 O. A. Melville, T. M. Grant, B. Mirka, N. T. Boileau, J. Park and B. H. Lessard, *Adv. Electron. Mater.*, 2019, **5**, 1900087.
28 O. A. Melville, T. M. Grant, K. Lochhead, B. King, R. Ambrose, N. A. Rice, N. T. Boileau, A. J. Peltekoff, M. Tousignant, I. G. Hill and B. H. Lessard, *ACS Appl. Electron. Mater.*, 2020, **2**, 1313–1322.
29 A. J. Pearson, T. Plint, S. T. E. Jones, B. H. Lessard, D. Credgington, T. P. Bender and N. C. Greenham, *J. Mater. Chem. C*, 2017, **5**, 12688–12698.
30 T. Plint, B. H. Lessard and T. P. Bender, *J. Appl. Phys.*, 2016, **119**, 145502.
31 T. M. Grant, T. Gorisse, O. Dautel, G. Wantz and B. H. Lessard, *J. Mater. Chem. A*, 2017, **5**, 1581–1587.
32 H. Raboui, A. J. Lough, T. Plint and T. P. Bender, *Cryst. Growth Des.*, 2018, **18**, 3193–3201.
33 B. King, O. A. Melville, N. A. Rice, S. Kashani, C. Tonnelé, H. Raboui, S. Swaraj, T. M. Grant, T. McAfee, T. P. Bender, H. Ade, F. Castet, L. Muccioli and B. H. Lessard, *ACS Appl. Electron. Mater.*, 2021, **3**, 325–336.
34 A. N. Fernandes and T. H. Richardson, *Colloids Surf., A*, 2006, **284–285**, 335–338.
35 P. D. Jeffery and P. M. Burr, *Sens. Actuators*, 1989, **17**, 475–480.

Open Access Article. Published on 30 April 2025. Downloaded on 8/16/2025 7:57:06 PM.
This article is licensed under a Creative Commons Attribution-NonCommercial 3.0 Unported Licence.

36 S. Ganesh Moorthy, B. King, A. Kumar, E. Lesniewska, B. H. Lessard and M. Bouvet, *Adv. Sens. Res.*, 2023, **2**, 2200030.
37 M. Polyakov, V. Ivanova, D. Klyamer, B. Köksoy, A. Şenocak, E. Demirbaş, M. Durmuş and T. Basova, *Molecules*, 2020, **25**, 1–17.
38 S. I. Büyükekşi, S. Z. Topal and D. Atilla, *J. Fluoresc.*, 2017, **27**, 1257–1266.
39 B. Şahin, S. Z. Topal and D. Atilla, *J. Fluoresc.*, 2017, **27**, 407–416.
40 A. G. Gürek, V. Ahsen, F. Heinemann and P. Zugenmaier, Molecular Crystals and Liquid Crystals Science and Technology. Section A, *Mol. Cryst. Liq. Cryst.*, 2000, **338**, 75–97.
41 T. V. Basova, A. G. Gürek and V. Ahsen, *Mater. Sci. Eng. C*, 2002, **22**, 99–104.
42 S. Dabak, V. Ahsen, F. Heinemann and P. Zugenmaier, *Mol. Cryst. Liq. Cryst. Sci. Technol., Sect. A*, 2000, **348**, 111–127.
43 D. Atilla, G. Aslibay, A. G. Gürek, H. Can and V. Ahsen, *Polyhedron*, 2007, **26**, 1061–1069.
44 M. M. El-Nahass, Z. El-Gohary and H. S. Soliman, *Opt. Laser Technol.*, 2003, **35**, 523–531.
45 T. J. Dines, *Polym. Int.*, 1993, **31**, 113–114.
46 B. M. Hassan, H. Li and N. B. McKeown, *J. Mater. Chem.*, 2000, **10**, 39–45.
47 T. V. Basova, M. Durmuş, A. Gül Gürek, V. Ahsen and A. Hassan, *J. Phys. Chem. C*, 2009, **113**, 19251–19257.
48 T. V. Basova, V. G. Kiselev, V. A. Plyashkevich, P. B. Cheblakov, F. Latteyer, H. Peisert and T. Chassè, *Chem. Phys.*, 2011, **380**, 40–47.
49 R. B. Ewenike, Z. S. Lin, R. R. Cranston, H. R. Lamontagne, A. J. Shuhendler, C.-H. Kim, J. L. Brusso and B. H. Lessard, *Adv. Funct. Mater.*, 2024, **34**, 2408779.
50 R. R. Cranston, T. D. Lanosky, R. Ewenike, S. Mckillop, B. King and B. H. Lessard, *Small Sci.*, 2024, **4**, 2300350.
51 M. Wang, Y. L. Yang, K. Deng and C. Wang, *Chem. Phys. Lett.*, 2007, **439**, 76–80.
52 A. D. Gülmez, M. S. Polyakov, V. V. Volchek, S. T. Kostakoğlu, A. A. Esenpinar, T. V. Basova, M. Durmuş, A. G. Gürek, V. Ahsen, H. A. Banimuslem and A. K. Hassan, *Sens. Actuators, B*, 2017, **241**, 364–375.
53 M. Ariyoshi, M. Sugibayashi-Kajita, A. Suzuki-Ichihara, T. Kato, T. Kamei, E. Itoh and K. Ohta, *J. Porphyrins Phthalocyanines*, 2012, **16**, 1114–1123.
54 Z. Zhao, P.-S. Chan, H. Li, K.-L. Wong, R. N. S. Wong, N.-K. Mak, J. Zhang, H.-L. Tam, W.-Y. Wong, D. W. J. Kwong and W.-K. Wong, *Inorg. Chem.*, 2012, **51**, 812–821.
55 O. A. Melville, B. H. Lessard and T. P. Bender, *ACS Appl. Mater. Interfaces*, 2015, **7**, 13105–13118.
56 A. N. Fernandes and T. H. Richardson, *J. Mater. Sci.*, 2008, **43**, 1305–1310.
57 T. M. Grant, N. A. Rice, L. Muccioli, F. Castet and B. H. Lessard, *ACS Appl. Electron. Mater.*, 2019, **1**, 494–504.
58 F. I. Bohrer, A. Sharoni, C. Colesniuc, J. Park, I. K. Schuller, A. C. Kummel and W. C. Trogler, *J. Am. Chem. Soc.*, 2007, **129**, 5640–5646.
59 A. Kumar, A. Singh, A. K. Debnath, S. Samanta, D. K. Aswal, S. K. Gupta and J. V. Yakhmi, *Talanta*, 2010, **82**, 1485–1489.
60 B. R. Kaafarani, *Chem. Mater.*, 2011, **23**, 378–396.
61 S. Ganesh Moorthy, B. King, A. Kumar, E. Lesniewska, B. H. Lessard and M. Bouvet, *Adv. Sens. Res.*, 2023, **2**, 1–13.
62 B. King, S. G. Moorthy, E. Lesniewska, R. Meunier-Prest, M. Bouvet and B. H. Lessard, *Sens. Actuators, B*, 2024, **408**, 135507.
63 H. Karakaş, V. Ivanova, G. G. Çelik, D. Atilla, A. G. Gürek, D. Klyamer and T. Basova, *Synth. Met.*, 2021, **281**, 116924.
64 V. Ivanova, D. Klyamer, G. Tunç, F. D. Gürbüz, D. Atilla, A. G. Gürek, A. Sukhikh and T. Basova, *New J. Chem.*, 2023, **47**, 19633–19645.
65 K. H. Kim, S. A. Jahan and E. Kabir, *TrAC, Trends Anal. Chem.*, 2012, **33**, 1–8.

 This journal is © The Royal Society of Chemistry and the Centre National de la Recherche Scientifique 2025